Proceedings of COBEM 2005
18th International Congress of Mechanical Engineering
November 6-11, 2005, Ouro Preto, MG


# A SINGLE DOF HAPTIC INTERFACE FOR COMPUTER INTERACTION

**Adriano Jotadiemel Masi, Marcelo Fernándes de Barros Cabaleiro**
Instituto Politécnico da Pontifícia Universidade Católica de Minas Gerais
Engenharia Eletrônica e de Telecomunicação – Av. Dom José Gaspar, 500 – Belo Horizonte – MG – 30535.610
amasi@uai.com.br, cabaleiro@yahoo.com

**Denilson Laudares Rodrigues**
Instituto Politécnico da Pontifícia Universidade Católica de Minas Gerais
Av. Dom José Gaspar, 500 – Belo Horizonte – MG – 30535.610
denilsonlr@pucminas.br

**Samir Araújo de Souza**
Ciência da Computação – Instituto de Informática da Pontifícia Universidade Católica de Minas Gerais
Av. Dom José Gaspar, 500 – Belo Horizonte – MG – 30535.610
samir.araújo@linuxmail.org

***Abstract.*** *Haptic interaction is enabled by a special sensor modality that combines sensing and action. The energy and information flow is bi-directional, so that, as the user touches and manipulates objects, he/she simultaneously changes their state and receives information about them. In our interactions with the world, haptics adds not only a compelling dimension to the information we receive, but also another means for expressiveness in our actions as well. The design of haptic interfaces to simulate virtual or real environments is a challenging problem in robotics, human-machine interface and computer graphics. The dynamic interactions among the human operator, the mechanism, sensors, actuators, the physic-based simulation, and the evaluation of the overall system bring interesting questions and important practical concerns. The focus of this work is on the design and implementation of simple haptic interface with a single degree-of-freedom. The goal was to design and to build a haptic interface that allows the simulation of virtual environments being able to be use in teleoperation applications. Based on the desired specifications for the haptic device, we implemented the mechanical prototype, the electronics, the control algorithms and the virtual environment to build our haptic interface.*

***Keywords***: *haptics, virtual environment, computer interaction*

## 1. Introduction

As a natural step beyond the dream of interacting with virtual worlds, enabled by today computers, the ever increasing development of new technologies has ushered in a new research area, which has been named "Haptics"[1]. Haptic interfaces are systems that provide kinesthetic and force feedback information to the user through physical interaction, enabling a realistic perception of virtual or real remote environments. Many authors use the word haptic to describe the use of hands and tactile sensibility to explore and manipulate the environment. Haptic systems, which are composed of mechanical, electronic, and software, are controlled by the human contact forces and may be programmed to elicit to the user the sensation of forces and torques associated with different environments, real or virtual.

Recently, haptic interfaces have become a reality that emerged from the synergy among the areas of robotics, computer vision and computer graphics (Ansar, 2001; Massie, 1994; Colgate, 1995; Burdea, 1996; Basdogan, 1999; Yokokohji, 1999; Hollerbach, 2000). This has allowed the deployment of powerful immersive tools. A haptic interface has two basic functions: to measure positions/forces (and their time derivatives) at the user's interaction port and to display forces/positions back to the user (human operator, as depicted in Figure 1). The user's interaction port is the region where the user touches the haptic device and where the energy is exchanged between the user and the haptic device. Figure 1 presents a generic diagram of a haptic interface. Broadly speaking, a haptic interface is composed of a haptic device and a computer, which runs algorithms to simulate virtual environments – the *Environment Simulator*, and also controls the haptic device – *Control System*, as presented in Figure 1.

A *Haptic device*, as one of the fundamental components of a haptic interface, is a mechanical structure with actuators and sensors that is used to capture the user's movements (position and orientation) and is able to apply forces and torques back to the user as a feedback of the interaction with a synthesized environment, or real.

*Haptic rendering* is the process of providing display to the sense of touch, by setting the stimulus, which correspond to the physical entities being displayed by a haptic device. The goal of haptic rendering, which is analogous to the techniques used in video or image display – thus render – images, is to enable a realistic perception of touch when immersed in an environment which may be built of virtual and/or real objects. Typically, a haptic rendering algorithm is composed of two main parts: *collision detection* and *collision response*. As the user manipulates the probe of a haptic

[1] "Haptic" comes from the Greek word *haptesthai* which means related to, or based on the sense of touch or tactile feedback (Webster, 1985)

device, new positions and orientations of the haptic probe are acquired and collisions with virtual objects are detected. If a collision is detected, interaction forces are computed using a priori defined rules and models for collision response. All these stimuli are conveyed to the user through the haptic device in order to provide him with the tactile "appearance" of 3-D objects as well as their surface features. The design of a haptic interface is a complex task, since it involves mechanical design, control architecture, dynamic interaction and visual display.

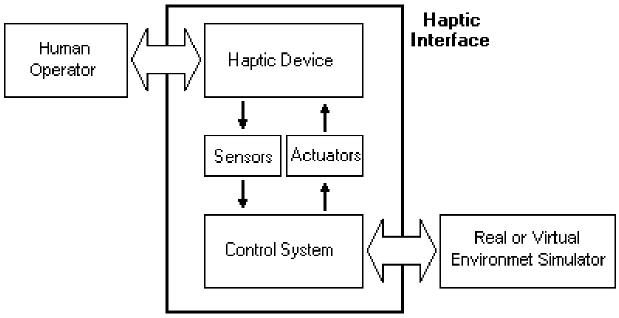


Figure 1. Generic block diagram for haptic interfaces.

With the introduction of high-fidelity haptic devices, it is now possible to simulate to the human perception system the feeling of smooth surface textures on complex shapes under dynamic conditions (Ho, 1999). Just as computer graphics is concerned with synthesizing and rendering visual images, *computer haptics* is the science of developing software algorithms that synthesize computer generated forces to be displayed to the user for perception and manipulation of virtual objects through touch (Basdogan, 1999).

This paper describes a design of a single degree-of-freedom haptic interface, used initially as force feedback device. The focus is on the design, implementation and evaluation of the different parts of such device.

**2. The Haptic Device Design**

The haptic device implemented was designed to be a low cost device, simple to be manufactured and assembled. The main goal in the design phase was to obtain a prototype of a force feedback joystick with a single degree-of-freedom.

This work applies the framework presented by Rodrigues (2002), addressing the issues for haptic device design. As pointed at Section 2, the goals in the mechanical design were:

1. High backdriveability - Looking the work done so far, the consensus seems to be that the "ideal" haptic interface device is one that is highly backdriveable. This is an important characteristic because it is necessary a maximum reality during the haptic task. This is a mechanical feature, which allows a mechanism to be driven either at its input or its output. Backdriveability is indispensable for a haptic device, since forces that are applied to its output needs to be transferred back to its inputs. Since haptic interfaces are used both as input and output devices, high backdriveability is not only necessary but it is the main mechanical feature of a haptic device.
2. Inertia - Another important characteristics to haptic device is low inertia. This because the user must feel his hand free in the space when he is moving the haptic device in free space. If the haptic device has a heavy mechanical structure, the user won't be able to move his hand in free space without feeling some reaction (inertia). Ideally, a haptic device should be transparent in the sense that throughout the interaction the user should perceive only the objects in the virtual environment. The larger inertia presented by the haptic device, the more it would degrade the rendering of the real object being displayed. A bulky mechanical structure will inevitably provide jerky motions to the user, which would be clearly sensed in the free space displacements. Keeping inertia at a minimum is of fundamental importance to the design of a haptic device.
3. Backlash - Backlash is usually present in most mechanisms driven by geartrains, which is the case of several commercial robots. Backlash introduces non-linearities that would greatly hinder the overall performance of the device, and therefore mechanisms should be carefully chosen and implemented and fine tuned to remove all backlash. As a robot, we do not want backlash in the mechanical structure. The shaft of the motors and mobile parts must be rigidly attached.
4. Internal friction - Friction within the haptic device is another important feature, since like backlash, it constitutes a non-linear mechanical phenomenon that has to be brought to a minimum. As a non-linear effect, the friction will be a noise during the task execution. In order to simulate free space, we have to take care about this characteristics. Friction that is typically present in all mechanical moving parts within a haptic device will greatly degenerate its performance and as a last resort. The control algorithm must carefully compensate it.
5. Force spectrum - Haptic tasks may range from flinging a light sheet of tissue paper in free space to a rough collision with a hard wall. In this case a large force range will be a important characteristics. Therefore a broad

range of force values needs to be correctly displayed. A broad force range is highly desirable. However, several issues make it difficult for the same haptic device to attain a very broad force range, which will dictate the feasible force limits achievable by the device.

6. Working volume - To use this haptic device for different applications a suitable working volume will be necessary. The working volume should be large enough, so it will not hinder the user's movements while performing a task. It may allow the use of the haptic device in as many different applications as possible.

Unfortunately simultaneously attaining all the features listed above can be conflicting. For instance, large force range and working volume require devices that are physically large, which normally implies in larger inertia, coupled friction and low bandwidth. In order to reach a good trade off among these criteria it is necessary to focus on the application (Clover, 1999). If the goal is to simulate gross dynamic forces and motion when manipulating a substantial mass, force range and working volume are key considerations, and force bandwidth becomes a secondary consideration. Otherwise, if it is desired to simulate fine motion of small mass and feel high frequency vibrations, then force bandwidth becomes a dominant criteria.

Figure 2 presents a CAD draw of the developed mechanical device. It has a base, a long radius arch and a finger support where the user holds. In the back side of the base, the DC motor is fixed. The motor shaft is attached to a steel cable, which is fixed to the long the radius arch. A steel cable is used to drive the arch. The user finger support is attached on the arch. This particular part of the haptic device is where the energy is changed between the users and the haptic device, and its called *user interaction port*.

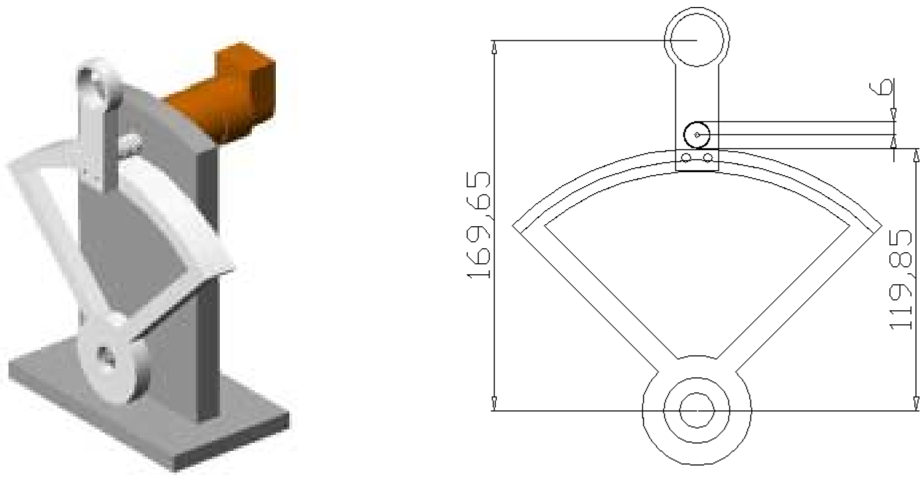


(a) (b)

Figure 2. Mechanical draws of the developed haptic device.

In order to reach the desired goals we chose the aluminum alloy 6351-T6, very common on the metal market. Its characteristics are present on Table 1.

Table 1. Physics properties of Al alloy 6351-T6 (Metals Handbook, 1990).

| **Physical Properties** | **Metric** | **Comments** |
|---|---|---|
| Density | 2710 kg/m$^3$ | AA; Typical |

| **Mechanical Properties** | **Metric** | **Comments** |
|---|---|---|
| Hardness, Brinell | 95 | AA; Typical; 500 g load; 10 mm ball |
| Hardness, Knoop | 130 | Converted from Brinell Hardness Value |
| Hardness, Rockwell A | 40 | Converted from Brinell Hardness Value |
| Hardness, Rockwell B | 60 | Converted from Brinell Hardness Value |
| Hardness, Vickers | 107 | Converted from Brinell Hardness Value |
| Ultimate Tensile Strength | 310 Mpa | AA; Typical |
| Tensile Yield Strength | 283 Mpa | AA; Typical |
| Elongation at Break | 14% | AA; Typical; 1.6 mm Thickness |
| Modulus of Elasticity | 68,9 Gpa | AA; Typical; Average of tension and compression. Compression modulus is about 2% greater than tensile modulus. |

| | | |
|---|---|---|
| Poisson's Ratio | 0,33 | Estimated from trends in similar Al alloys. |
| Fatigue Strength | 89,6 Mpa | AA; 500,000,000 cycles completely reversed stress; RR Moore machine/specimen |
| Shear Modulus | 26 Gpa | Estimated from similar Al alloys. |
| Shear Strength | 200 Mpa | AA; Typical |

In the motor shaft the pulley has $r_p$ = 6,00mm, the arch has $r_a$ = 119,85mm and the handle $r_h$ = 169,65mm, as presented at Figure 2. In the mechanical movement transmition we have

$$\frac{\omega_p}{\omega_a} = \frac{T_a}{T_p} = \frac{r_a}{r_p}, \tag{1}$$

where $\omega_a$ is the angular velocity of the arch, $\omega_p$ is the angular velocity of the pulley, $T_a$ is the torque on the arch, $T_p$ is the torque on the pulley. So, rewriting Equation (1), we have

$$T_a = T_p \frac{r_a}{r_p}. \tag{2}$$

We know that pulley torque is equal motor torque ($T_p$=$T_m$). Rewriting (2):

$$T_a = T_m \frac{r_a}{r_p}. \tag{3}$$

From the motor modeling we have:

$$T_m = k_m I_a, \tag{4}$$

where $k_m$ is the torque constant and $I_a$ is the armature current. It was specified a DC motor from Faulhaber, the 3557K 024CR (Faulhaber, 2000), based on the desired characteristics for the designed haptic device. Evaluating the maximum force in the handle, $F_h$ by using the motor's specifications (Table 2) we have:

$$T_{m_{\max}} = 0{,}0429\ \mathrm{Nm}/\mathrm{A} \cdot 2\ \mathrm{A} = 0{,}0858\ \mathrm{Nm} \tag{5}$$

$$T_{a_{\max}} = 0{,}0858\ \mathrm{Nm} \cdot \frac{119{,}85\times10^{-3}\ \mathrm{m}}{6\times10^{-3}\ \mathrm{m}} = 1{,}714\ \mathrm{Nm} \tag{6}$$

$$T_{a_{\max}} = F_{h_{\max}} \cdot r_h \tag{7}$$

$$F_{h_{\max}} = \frac{1{,}714\ \mathrm{Nm}}{169{,}65\times10^{-3}\ \mathrm{m}} = 10{,}10\ \mathrm{N} \tag{8}$$

By using the designed haptic device, we will be able to simulate forces up to 10N during a haptic simulation (environment exploration, teleoperation, virtual environment interaction).

Table 2. Motor Faulhaber 3557K CR024 specifications.

| Parameter | Value |
|---|---|
| Nominal voltage | 24,0 V |
| Terminal resistance | 2,0 Ohms |
| Output power | 70,8 W |
| Efficiency | 83 % |
| No-load speed | 5300 rpm |

| | |
|---|---|
| No-load current | 0,10 A |
| Stall torque | 510 mNm |
| Friction torque | 4,3 mNm |
| Speed constant | 223 rpm/V |
| Back-EMF constant | 4,49 mV/rpm |
| Torque Constant | 42,90 mNm/A |
| Current constant | 0,023 A/mNm |
| Rotor inductance | 270 μH |
| Mechanical time constant | 7 ms |
| Rotor inertia | 64 gcm$^2$ |
| Angular acceleration | 0,079 rad/s$^2$ |
| Shaft bearings | Ball bearings preloaded |
| Current up to (thermal limits) | 1,95 A |

## 4. Electronics Design

In order to control the force applied on the user's finger it was necessary to design an electronic hardware. By using a Microchip microcontroller (Microchip, 2001) a microcontroled CPU was implemented. On this CPU, presented at Figure 3, a local controller takes care about the current value on the motor armature, consequently force on the user´s interaction port. It reports angular positions to a host computer by using the serial connection (Tocci, 1983). A DC/DC converter and a low pass filter were implemented on the electronics hardware, as presented at Figure 3. The microcontroller receives the force set-point from the host and inform positions and velocities of the user interaction port. The communication between the host and the microcontroller hardware was implemented by using the RS232C standard interface. To measure current values from the armature circuit, a shunt was used. To drive armature current we are using a DC/DC converter, controlled by the pulse-width-modulation (PWM) technique. These parts will be detailed in the next sub-sections.

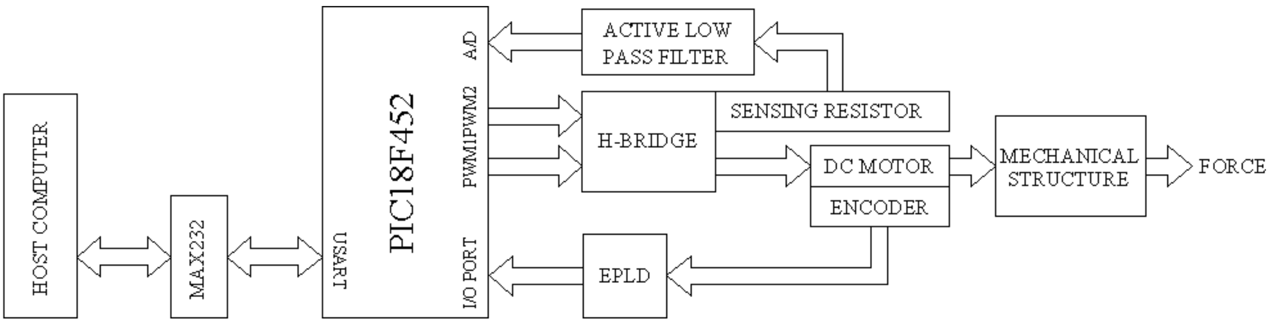


Figure 3. Block Diagram of the implemented electronic system.

### 4.1. Filter Design

To control the output force, it is necessary to control the motor current. After the power switches, the motor current is driven to a low value resistor (a 0,47ohms shunt resistor), where we can acquire the voltage signal that is proportional to the motor current. Once this signal is very noisy (mainly because the switching frequency of the chopper circuit), and also with a low magnitude, it was necessary to introduce an active linear filter before the AD converter. The voltage value over this shunt resistor is proportional to the current value, which is directly proportional to the motor torque, consequently, the output force. An active low pass Butterworth 4$^{th}$ order filter was designed, implemented and evaluated for this application (Willian, 1981). Figure 4 presents the active VCVS (Voltage-Controlled Voltage Source) Butterworth 4$^{th}$ order low pass filter used. As can be seen, the filter was implemented by cascading two 2$^{nd}$ order Butterworth filters.

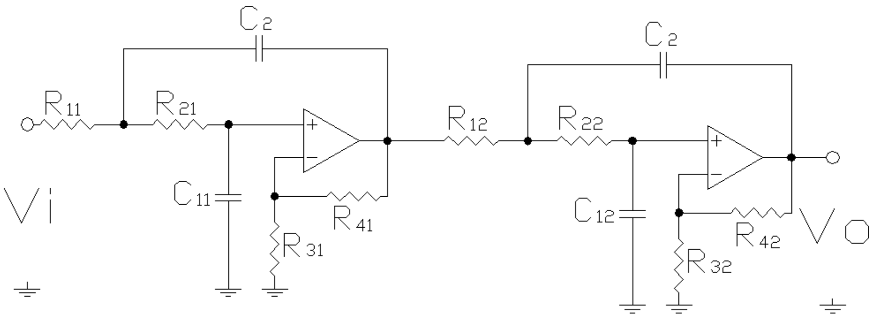


Figure 4. Fourth order Butterworth filter.

Figure 5 presents the experimental results of the implemented filter. It presents the Bode diagrams where the frequency response of the filter can be observed. The desired cut-off frequency was planned to 100hz and a 14dB bandwidth gain.

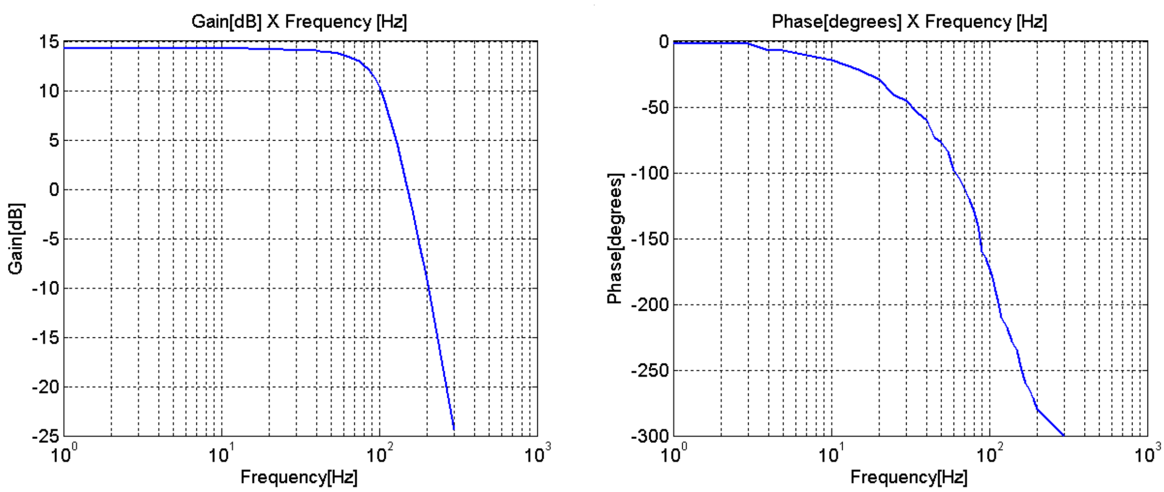


Figure 5. Experimental result of the implemented filter

### 4.2. Encoder Input

A digital encoder was used to inform the arch angular position. In order to make possible the integration of the encoder signals with the microcontroller a quadrature counter was implemented on the EPLD (Erasable Programmable Logical Device). This implementation introduced very good results because it is also multiply the encoder resolution by four. The implementation in VHDL (Hardware Description Language) is a state machine where the phase relationship between the A and B signals from the encoder were checked. Figure 6 presents the graphical representation of the encoder signals. Table 3 presents the states of the quadrature counter implemented.

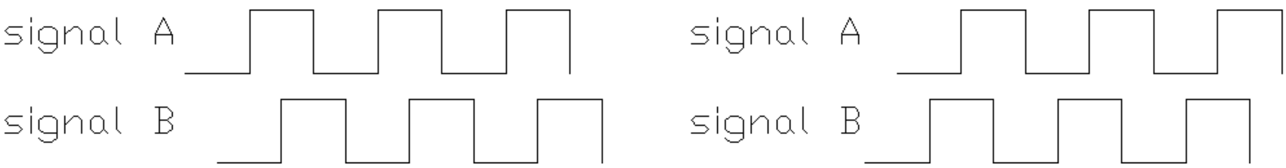


Figure 6. Encoder output signals: up and down count respectively.

The counter implemented make possible to multiply the resolution of the encoder by four, as can be seen at Table 3.

Table 3. Quadrature encoder: rules to count up and down.

| Count Up | Count Down |
|---|---|
| Positive edge of A and B=0 | Positive edge of A and B=1 |
| Positive edge of B and A=1 | Positive edge of B and A=0 |

| | |
|---|---|
| Negative edge of A and B=1 | Negative edge of A and B=0 |
| Negative edge of B and A=0 | Negative edge of B and A=1 |

### 4.3. Haptic Device Control

On the electronics hardware a digital PID controller is responsible to keep the current value as requested by the host. The design of the current control was implemented in Simulink and then, implemented on the microcontroller circuit board. The controller runs every 1ms, being able to handle dynamic effects of the system. The current controller was tuned by using the Zielger-Nichols methodology (Ogata, 2000). Bellow were presented the graph simulation on Simulink (Matlab®) at Figure 7, and the torque output at Figure 8.

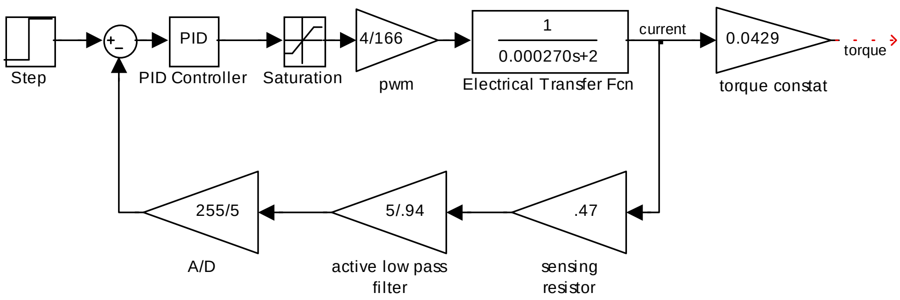


Figure 7. Graphical simulation scheme.

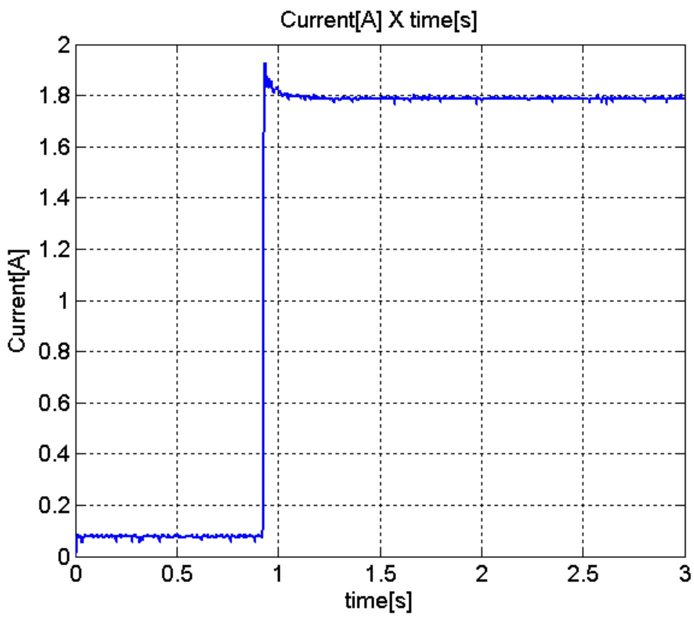


Figure 8. Armature current value for a step input.

## 5. Environment Simulator

A primary goal of virtual environment simulations, whether haptic or visual, is to achieve a sense of presence. Based on the information from the *Environment Simulator* and the position of the user's interaction port, the *Control System* on the host computer calculate forces that should be applied back to the user in order to simulate physical interaction. The position of the user interaction port is continually feed to the environment simulator by the microcontroller. Cohen presented a simpler and efficient algorithm to identify potential collisions using bounding boxes (Cohen *et al.*, 1995). By following his directions, a bounding box was defined as a larger square or regular polygon that contain the objects. This approach enclose all virtual objects of interest with bounding boxes. The axes of the bounding boxes are aligned with the world coordinate system. A bounding box can be considered to be static, when the boxes' dimensions remain constant independent of the orientation of the object, or dynamic, when its dimensions (but not its orientation) are adjusted as function of the orientation of the enclosed object in space. The approximate collision detection algorithm begins by projecting each bounding box onto the x, y and z world coordinate axes resulting in several intervals. A pair of bounding boxes overlaps if and only if their intervals in all three dimensions overlap. This can easily be checked for the one-dimensional case. He also implemented a two-dimensional test for projections in any two of the xy, xz and yz planes. Each of those projections is a rectangle in 2-D plane. Typically, there are fewer overlaps of those 2-D rectangles than of 1-D intervals. In situations where the projections onto one-dimension result in densely clustered intervals, the two-dimensional technique is shown to be more efficient.

**6. Conclusions**

The paper presents a single degree-of-freedom haptic system. The main goal of this work was the design and implementation of a haptic system. The main results, haptic device mechanical structure and electronics hardware, was presented. Many issues should be addressed until be able to do a real time simulation. Based on the mechanical properties of such device, or implementing an identification experiment to identify dynamic parameters, we will be able to improve the control of the mechanical structure. The controller design should be improved by using the device dynamical model and its parameters. For instance, we are able to simulate reaction forces as a mass-spring-damper system. Calibration procedures should be executed in order to add realism on the simulations. The haptic device was designed to apply until 8 kgf on the user´s hand (user interaction port). The Faulhaber motor is suitable for this application once has a high torque capability. The encoder answer was working fine, being able to report angular positions on 5kHz ratio.

**7. Acknowledgements**

Part of this work was carried out at Grupo de Estudos em Automação e Robótica of PUC Minas. The authors gratefully acknowledge the support from Marte Balanças, the Company that believed and helped in this project since the beginning.

**8. References**

Ansar, A., Rodrigues, D., Desai, J., Daniilidis, K., Kumar, V., and Campos, M. ; 2001. "Visual and haptic collaborative tele-presence". Elsevier Science Computers and Graphics, 25(5), pp 789-798.

Basdogan, C., 1999. "Force reflecting deformable objects for virtual environments. In SIGGRAPH. Tutorial Notes of 26th International Conference on Computer Graphics and Interative Techniques.

Burdea, G.C., 1996, "Force and touch feedback for virtual reality", John Willey & Sons, New York, NY, USA.

Clover, C.; 1999. "A control-system architecture for robots used to simulate dynamic force and moment interaction between human and virtual objects". IEEE Transactions on Systems, Man, and Cybernetics - Part C: Applications and Reviews, 29(4); pp 481-493.

Colgate, F.; Stanley, M.; Broen, J., 1995. "Issues in the haptic display of tool use". In Proceedings IEEE/RSJ International Conference Robots Systems.

Faulhaber, 2000. Miniature Drive System – Second Edition, Faulhaber Group.

Ho, C.; Basdogan, C.; Srinivasan, M., 1999. " Efficient point-based rendering Techniques for haptic display of virtual objects. Presence, Vo. 8, No. 5, pp 477-791.

Hollerbach, J., 2000. "Some current issues in haptics research". In proceedings of the International Conference on Robotics and Automation, pp 757-761.

Massie, T. and Salisbury, K., 1994. "The phanton haptic interface: A device for probing virtual objects". In ASME Annual Meeting, Vol. 55, ASME, pp 295-300.

Metals Handbook, 1990. Properties and Selection: Nonferrous Alloys and Special-Purpose Materials, Vol. 2. ASM International 10th Edition.

Microchip data sheet, 2001. "Micontroller PIC18F877 – user guide".

Ogata, K., 2000. "Teoria de controle moderno". LTC – Livros Técnicos e Científicos Ltda, Rio de Janeiro – RJ.

Rodrigues, D.L., 2002. "Projeto, implementação e avaliação de interfaces háticas", Tese de Doutorado, Departamento de Ciência da Computação – DCC – UFMG.

Yokokohji, Y., Hollis, R., Kanade, T., 1999, "Wysiwyf display: A visual/haptic interface to virtual environment", Presence, Vol. 8, no. 4, pp. 412-434.

Webster's Ninth New Collegiate Dictionary, 1985, Merriam-Webster Inc., Springfield, MA, USA

Willian, A.B., 1981. "Electronic Filter Design Handbook", McGraw-Hill Book Company, USA.

**9. Responsibility notice**